Investigation of Active Damping Approaches for PI-Based Current Control of Grid-Connected Pulse Width Modulation Converters With LCL Filters

Jörg Dannehl, *Student Member, IEEE*, Friedrich Wilhelm Fuchs, *Senior Member, IEEE*, Steffan Hansen, *Member, IEEE*, and Paul Bach Thøgersen, *Senior Member, IEEE*

***Abstract*—This paper deals with various active damping approaches for PI-based current control of grid-connected pulsewidth-modulation (PWM) converters with LCL filters, which are based on one additional feedback. Filter capacitor current, as well as voltage feedback for the purpose of resonance damping, are analyzed and compared. Basic studies in the continuous Laplace domain show that either proportional current feedback or derivative voltage feedback yields resonance damping. Detailed investigations of these two approaches in the discrete z-domain, taking into account the discrete nature of control implementation, sampling, and PWM, are carried out. Several ratios of LCL resonance frequency and control frequency are considered. At high resonance frequencies, only current feedback stabilizes the system. At medium resonance frequencies, both approaches have good performance. At low resonance frequencies, stability gets worse, even though voltage feedback offers slightly better damping properties. Measurements validate the theoretical results.**

***Index Terms*—Active resonance damping, current feedback, grid-connected PWM converter, LCL filter, PI current control, voltage feedback.**

I. Introduction

THREE-PHASE grid-connected pulsewidth-modulation (PWM) converters are often used in regenerative energy systems and in adjustable speed drives when regenerative braking is required [1]. Power regeneration, adjustable power factor, controllable dc-link voltage, and reduced line current harmonic distortion are its most important advantages over passive diode bridges. For the reduction of line current ripple, LCL filters are often used as grid filters [2]. Due to their high efficiency and flexibility, active resonance damping solutions as part of converter control have attracted much attention [3]–[8].

Converter control commonly consists of an outer dc-link voltage PI control loop and an inner current control loop. For some applications with line current feedback, the well-known PI control in the synchronous reference frame can be employed. However, the inner PI-based current control is not suitable for many applications, depending on the ratio of LCL resonance frequency to control frequency [9]. At lower ratios, converter current feedback PI control leads to instability. For these applications, active resonance damping gets integrated into the current control loop. Sensorless resonance damping [10], as well as damping with additional feedback, are presented in the literature. In [3], [4], [10], [11], resonance is damped with additional feedback of the voltages across the filter capacitors. In [12], [13], the current through the filter capacitors is used for resonance damping, and in [7], various solutions based on the so-called virtual resistors are presented. For certain system settings, the resonance damping effect is put into evidence and the control performance is analyzed. Analyses with different system settings, particularly different ratios of resonance and control frequency, are often not carried out. For this reason, one damping approach presented in [7] is analyzed in more detail in [14].

In this paper, a more general analysis of different resonance damping solutions is carried out. Basic LCL resonance damping properties of different feedback states are studied. The feedback of the current through or voltage across the LCL filter capacitors with different feedback transfer functions are considered and compared in the continuous Laplace domain. The results show how the various feedback signals need to be fed back in order to achieve resonance damping. Detailed investigations of the two most suitable damping approaches in the discrete z-domain, taking into account the discrete nature of control implementation, sampling, and PWM, follow the general analysis. Different ratios of LCL filter resonance and control frequency are analyzed. Active resonance damping performance suffers from practical issues. The limitations of approaches based on one additional feedback loop of the current through or voltage across the filter capacitors are shown and explained.

First, the system is described and a mathematical model is presented in Section II, then an overview of control is given in Section III. A basic study of damping properties is carried out

Manuscript received August 28, 2009; revised December 8, 2009; accepted January 12, 2010. Date of publication May 24, 2010; date of current version July 21, 2010. Paper 2009-IPCC-299.R1, presented at the 2009 IEEE Energy Conversion Congress and Exposition, San Jose, CA, September 20–24, and approved for publication in the IEEE Transactions on Industry Applications by the Industrial Power Converter Committee of the IEEE Industry Applications Society. This work was supported by the German Research Foundation (DFG) and Industry.

J. Dannehl and F. W. Fuchs are with the Institute for Power Electronics and Electrical Drives, Christian-Albrechts-University of Kiel, 24143 Kiel, Germany (e-mail: dannehl@ieee.org; fwf@tf.uni-kiel.de).

S. Hansen is with Danfoss Drives A/S, 6100 Graasten, Denmark (e-mail: s.hansen@danfoss.com).

P. B. Thøgersen is with KK-Electronic A/S, 9220 Aalborg, Denmark (e-mail: patho@kk-electronic.com).

Color versions of one or more of the figures in this paper are available online at http://ieeexplore.ieee.org.

Digital Object Identifier 10.1109/TIA.2010.2049974

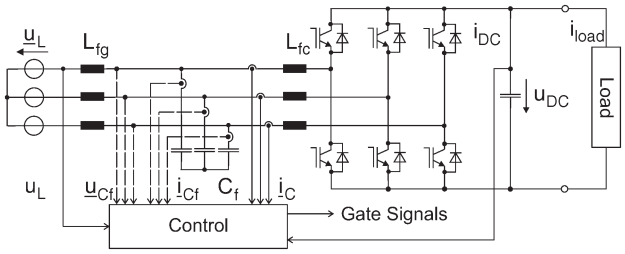

Fig. 1. Grid-connected PWM converter with LCL filter.

in Section IV. Practical issues are addressed in Section V. A detailed investigation of filter capacitor current feedback with different typical system settings is presented in Section VI-A, while filter capacitor voltage feedback is covered in Section VI-B. The results of measurements are presented in Section VII. Finally, a comparison and conclusion are given.

II. System Description

A three-phase IGBT voltage source converter is studied. It is connected to the grid via an LCL filter, as shown in Fig. 1. In addition to the dc-link voltage and converter currents, either the filter capacitor currents or filter capacitor voltages are measured. The line voltages are measured for the purpose of synchronizing the control with the line voltage. The converter is loaded by an inverter-fed induction machine. In this paper, several filter capacitances are used in order to study different ratios of resonance and control frequency.

Applying Kirchhoff's laws yields the continuous model of the LCL filter (u_C: converter output voltage) [9]

$$\begin{aligned}
\frac{d}{dt}\overset{i\,dq}{\rightarrow}_L &= \frac{1}{L_{fg}}\cdot\left(\overset{u\,dq}{\rightarrow}_L - \overset{u\,dq}{\rightarrow}_{Cf}\right) - j\omega\cdot\overset{i\,dq}{\rightarrow}_L \\
\frac{d}{dt}\overset{i\,dq}{\rightarrow}_C &= \frac{1}{L_{fc}}\cdot\left(\overset{u\,dq}{\rightarrow}_{Cf} - \overset{u\,dq}{\rightarrow}_C\right) - j\omega\cdot\overset{i\,dq}{\rightarrow}_C \\
\frac{d}{dt}\overset{u\,dq}{\rightarrow}_{Cf} &= \frac{1}{C_f}\cdot\left(\overset{i\,dq}{\rightarrow}_L - \overset{i\,dq}{\rightarrow}_C\right) - j\omega\cdot\overset{u\,dq}{\rightarrow}_{Cf}\,.
\end{aligned} \tag{1}$$

The resonance frequency of the LCL filter can be calculated as

$$\omega_{\mathrm{Res}} = \sqrt{\frac{L_{fg}+L_{fc}}{C_f L_{fg} L_{fc}}}. \tag{2}$$

Because the outer dc-link voltage is outside the scope of this paper, the reader is referred to [9] for a mathematical description of dc-link dynamics and control. From (1), the transfer function $G_{\mathrm{LCL}}^{Ucf}(s)$ can be derived

$$G_{\mathrm{LCL}}^{Ucf}(s) = \frac{U_{Cf}(s)}{U_C(s)} = \frac{1}{L_c C_f}\frac{1}{s^2+\omega_{\mathrm{Res}}^2} \tag{3}$$

and taking into account $I_{Cf}(s) = sC_f U_{Cf}(s)$, this gives

$$G_{\mathrm{LCL}}^{Icf}(s) = \frac{I_{Cf}(s)}{U_{Cf}(s)}\cdot\frac{U_{Cf}(s)}{U_C(s)} = \frac{1}{L_c}\frac{s}{s^2+\omega_{\mathrm{Res}}^2}. \tag{4}$$

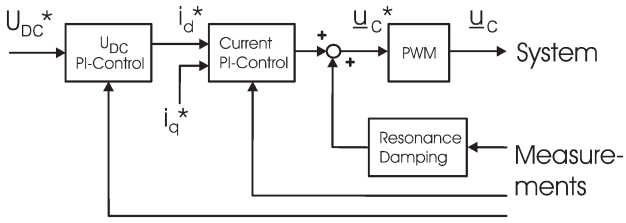

Fig. 2. Cascaded control structure including resonance damping based on additional feedback.

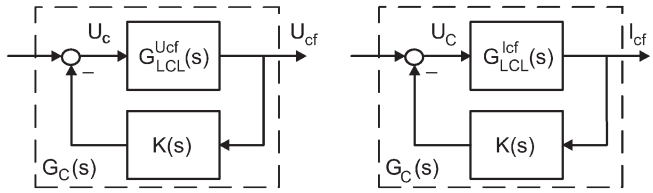

Fig. 3. Feedback of (left) filter capacitor voltage and (right) filter capacitor current.

III. Control Overview

The control structure is shown in Fig. 2. The dc-link voltage is controlled with a PI controller [9]. Active and reactive converter currents are controlled in the synchronous reference frame with PI controllers. In this paper, converter current control is employed. Similar analyses can be carried out on line current control. Control is executed at a control frequency f_c and sampling is carried out at the same frequency. The proportional gain k_p and the integrator time constant T_I of the PI controllers are tuned according to symmetrical optimum [15], whereas the L filter approximation of the LCL filter is used [16] ($T_c = 1/f_c$)

$$k_p = -\frac{L_{fg}+L_{fc}}{3\cdot T_c} \quad T_I = 9\cdot T_c. \tag{5}$$

With this PI tuning and backwards implementation [17], the response to a reference step shows an overshoot of approximately 30% and the reference is crossed after approximately 3 to 4 control periods. Note that more stringent requirements with respect to overshoot could be fulfilled by different tuning. In addition, feedforward decoupling is employed [9] Fig. 3.

For the LCL filter system, active resonance damping is required. Sensorless resonance damping is possible [18], but it has been shown to be rather sensitive to parameter variations [8]. Moreover, it cannot be applied to every kind of LCL filter design [9]. Applying additional feedback to the system offers improvements. Various solutions can be found in the literature. In this paper, a more generic study of the approaches adopted to dampen resonance by feeding back one additional state variable is carried out.

IV. Basic Study of Resonance Damping With Different Feedback States

As the resonance is caused by the filter capacitors, it is reasonable to use the current through them or voltage across them for the purpose of resonance damping. Which kind of sensor to choose depends strongly on the application, as well

TABLE I
CLOSED-LOOP TRANSFER FUNCTIONS WITH U_{Cf} AND I_{Cf} FEEDBACK FOR DIFFERENT FEEDBACK TYPES

Feedback type	$G_c(s)$ for U_{Cf} feedback	$G_c(s)$ for I_{Cf} feedback
$K(s) = K$ (P-type)	$\frac{1}{L_c C_f} \; \frac{1}{s^2 + (\omega_{Res}^2 + K/(L_c C_f))}$	$\frac{1}{L_c} \; \frac{s}{s^2 + s \underbrace{(K_{iCf}/(L_c)}_{damping} + \omega_{Res}^2}$
$K(s) = K\,s$ (D-type)	$\frac{1}{L_c C_f} \; \frac{1}{s^2 + s \underbrace{K/(L_c C_f)}_{damping} + \omega_{Res}^2}$	$\frac{1}{L_c + K_{iCf}} \frac{s}{s^2 + \left(\frac{L_c}{L_c + K_{iCf}}\right) \omega_{Res}^2}$
$K(s) = \frac{K}{s}$ (I-type)	$\frac{1}{L_c C_f} \; \frac{s}{s^3 + s\omega_{Res}^2 + K/(L_c C_f)}$	$\frac{1}{L_c} \; \frac{s}{s^2 + \left(K_{iCf}/L_c + \omega_{Res}^2\right)}$

as on the voltage and current level. For higher power/current levels (MW range, but at low voltages $<$ 1000 V ac) current sensors are much more expensive than voltage sensors. At low power (few kW range), standard current sensors might even be cheaper than voltage sensors with the same level of insulation. In the lowest power/current range, where the power circuit typically is integrated on a PCB, other issues (such as use of PCB area) might be important cost drivers. Moreover, in some applications, voltage sensors are used anyway for grid synchronization [3]. The number of sensors can also be reduced by estimating some of the feedback signals [4]. In this paper, the resonance damping properties of both types of feedback signal are studied.

The influence of filter capacitor current or voltage feedback on the system poles is studied separately. The analysis is carried out in the continuous Laplace domain. For this purpose, delays caused by PWM and computation, as well as discretization effects, are neglected at this stage. More detailed analyses are presented later in Section VI. The loops illustrated in Fig. 2 are analyzed, whereas different feedback transfer functions $K(s)$ are taken into consideration, namely proportional, derivative, and integral feedback. The closed-loop transfer function $G_c(s)$ can be calculated as

$$G_c(s) = \frac{G_{\mathrm{LCL}}(s)}{K(s) + G_{\mathrm{LCL}}(s)} \tag{6}$$

whereas for U_{Cf} feedback (3) is used and (4) for I_{Cf} feedback.

In this paper, feedback on the converter voltage references is considered. Note that feedback on the current references, instead of voltage references, is also possible. This can be beneficial with respect to current overshoot during transients [6]. In [7], [14], this is used as part of the concept of a so-called virtual resistor. In [6], it is used as part of deadbeat state space control. Similar analyses including a PI controller in the loop give the required types of feedback. As this is beyond the scope of this paper, results are not shown here.

A. Filter Capacitor Voltage Feedback

Evaluations of (3) and (6) for various types of feedback are shown in Table I. For proportional feedback, the transfer function of a resonator is obtained, whereas the natural resonance frequency ω_{Res} is shifted in proportion with K. As can be seen in Fig. 4, the complex conjugate poles are shifted along the imaginary axis in proportion with the proportional gain. Thus, no resonance damping is achieved by proportional feedback of the filter capacitor voltage.

Derivative feedback gives a second-order delay transfer function. The natural resonance frequency ω_{Res} remains but a nonzero damping factor is obtained, which is the term related to s. The complex conjugate poles are shifted into the left half of the s-plane in proportion with the derivative gain. Thus, resonance damping is achieved by the derivative feedback of the filter capacitor voltage with no frequency shift.

From Fig. 4, it can be seen that the system poles are shifted into the right half of the s-plane in the case of integral feedback. Thus, the system becomes unstable with integral feedback.

It can be concluded that derivative filter capacitor voltage feedback is required for resonance damping. Approaches in the literature using the filter capacitor voltage for resonance damping basically follow this result. In [3], [10], the voltage is fed back with a lead element which exhibits high-pass characteristics. In [4], a high-pass filter is directly selected from the start. As will be shown later, the discrete differentiator can also be regarded as a high-pass filter.

B. Filter Capacitor Current Feedback

Based on the result of the previous section, it can be expected that the proportional I_{Cf} feedback yields resonance damping, as $I_{Cf}(s) = sC_f U_{Cf}(s)$ holds. The pole zero maps in Fig. 4 and the transfer functions in Table I confirm this expectation. Approaches in the literature using the filter capacitor current for resonance damping follow this result. In [12], [13], proportional feedback is used.

V. PRACTICAL ISSUES

From the analysis based on simplified continuous models in the previous section, it is clear that the proportional I_{Cf} feedback and/or derivative U_{Cf} feedback yield resonance damping. However, there are various practical issues which influence the damping performance.

First of all, it is part of a digital control system. Hence, active resonance damping is only possible if its frequency is below the Nyquist frequency, which is half the control frequency [19]. Moreover, the resonance damping functionality is integrated

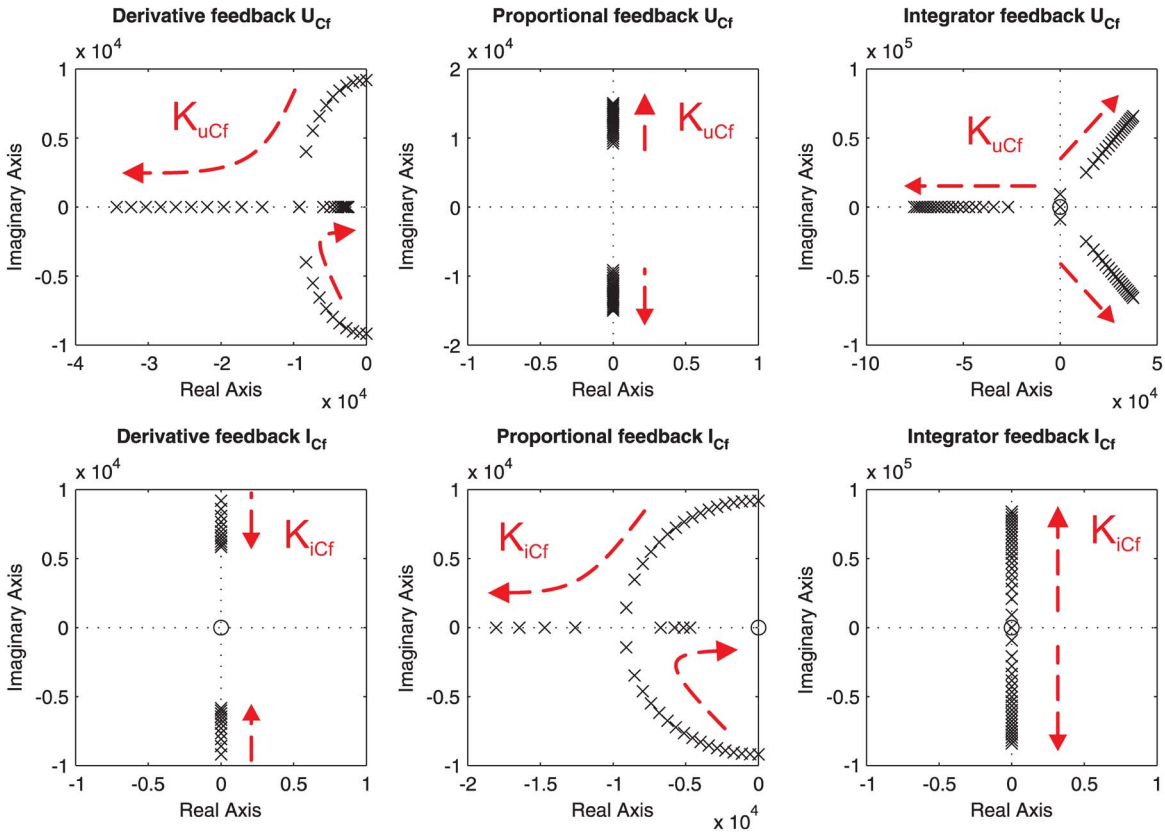

Fig. 4. Impact of different continuous feedback characteristics on the system pole-zero locations in the continuous s-plane (PWM neglected): (top) Filter capacitor voltage feedback and (bottom) filter capacitor current feedback.

into the current control loop. Both the fundamental PI current controller and the resonance damping part act on the same current dynamic. As they interact with each other, performance and stability may suffer, particularly when the resonance frequency comes close to the closed-loop controller bandwidth of the fundamental control.

Another point is the discrete implementation of the dynamic U_{Cf} feedback. The frequency behavior of differentiators discretized with forward difference, backward difference, Tustin approximation [17] and a continuous differentiator are shown in Fig. 5. Even though the Tustin approximation gives a perfect match of phase, the deviations in magnitude close to the Nyquist frequency are high. Root loci that are not shown in this paper indicate that the overall control system gets unstable in any case if the Tustin approximation is used. In terms of magnitude, forward and backward discretization yield better matches than Tustin. However, deviations in phase occur: $\pm 90^\circ$ at the Nyquist frequency. As forward discretization gives an implicit control algorithm, backward discretization is used here: $K(z) = K_{uCf} \cdot C_f(1 - z^{-1})/T_c$. Fig. 5 shows that, with increasing frequency, the characteristic of the backward differentiator changes from a differentiator to proportional gain, with constant magnitude and zero phase. On one hand, this is good as noise amplification is limited, but on the other hand, the derivative character that is required disappears at higher frequencies.

In practice, the LCL filter resonance is naturally damped by parasitic copper and iron losses. For efficiency reasons, they are

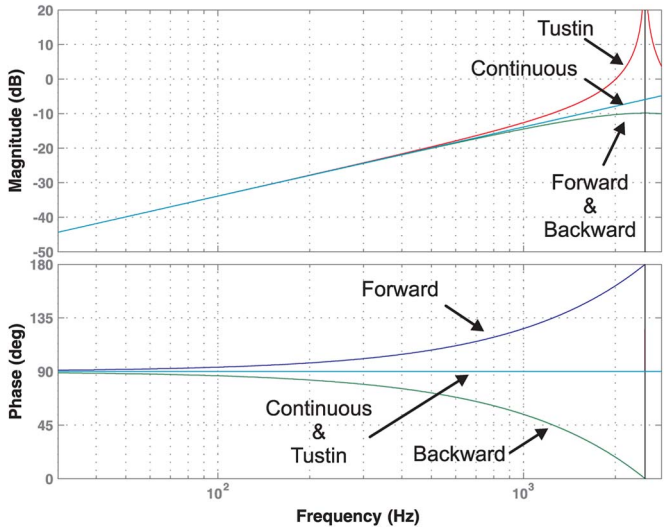

Fig. 5. Impact of discretization method on the frequency characteristic of the approximated differentiators in comparison to the continuous one.

kept low at a reasonable level. For higher power applications, they may even be negligible. Anyway, as the losses are not counteracting the active damping effect, only small parasitic winding resistances are taken into account. More detailed studies related to losses can be found in [9], [20].

The main disturbances in the current control loop are background line voltage harmonics and aliasing effects. The first is a well-known problem and manifold solutions have been

TABLE II
SYSTEM PARAMETERS

Symbol	Quantity	Value
U_L	Line voltage (phase-to-phase, rms)	400 V
ω	Line angular frequency	2 π 50 Hz
U_{DC}	DC-link voltage	700 V
P	Nominal power (grid-side)	25 kW
f_c	Switching/control frequency	2.5 / 5kHz
C_{DC}	DC-link capacitance	2710 μF

TABLE III
LCL FILTER SETTINGS AND CORRESPONDING RESONANCE FREQUENCIES

Setting	C_f/μF (p.u.)	L_{fg}/mH (p.u.) $R_{fg}/\text{m}\Omega$ (p.u.)	L_{fc}/mH (p.u.) $R_{fc}/\text{m}\Omega$ (p.u.)	f_{Res}/ kHz
I	16.3 (3.25 %)	0.75 (3.7 %) 50 (0.79 %)	2.0 (9.9 %) 60 (0.95 %)	1.69 (high)
II	32.6 (6.5 %)	0.75 (3.7 %) 50 (0.79 %)	2.0 (9.9 %) 60 (0.95 %)	1.19 (medium)
III	97.8 (19.5 %)	0.75 (3.7 %) 50 (0.79 %)	2.0 (9.9 %) 60 (0.95 %)	0.69 (low)

proposed [2], [21]. The second originates in sampling currents and voltages that are distorted by switching harmonics and multiples. Sampling the signals during zero converter output voltage vectors eliminates most of the switching distortions and is done typically. Further aliasing reduction can be obtained by either analog filtering or by digital filtering of oversampled signals [22]. However, resonance damping properties are emphazised in this paper and disturbance rejection is beyond the scope of this paper and not treated any further.

VI. DETAILED ANALYSIS OF OVERALL DIGITAL CURRENT CONTROL SYSTEM

In the following detailed study, a typical system setting for a medium power drive is selected (see Table II). In order to cover a typical range of LCL filter parameters, three different LCL filter settings are studied. The choice of filter elements is a tradeoff between switching harmonics attenuation, reactive power consumption, relative short-circuit voltage drop, grid decoupling, filter losses, as well as the costs and sizes of filter elements. Research on LCL filter design is documented in [16], [23]. From the control and resonance damping points of view, the ratio of resonance frequency to control frequency is the most important. Therefore, the control is analyzed in detail for three characteristic ratios. In this paper, the control frequency is kept constant and the resonance frequency is varied by changing the filter capacitance. The inductances are not changed. Table III shows the LCL filter parameter settings selected for the following analyses. Settings are classified into high, medium, and low resonance frequencies. The results can easily be transferred to other LCL filter settings and switching frequencies. The models used for system analysis are shown in Fig. 6. A consideration of the sampling process leads to an analysis in the discrete z-domain. The continuous LCL filter model is discretized by a zeroth-order hold method [17]. Moreover, the parasitic series resistances of the inductors are taken into account, but the parallel resistances that model core losses are neglected. The coupling terms in (1) are neglected and the analysis is done for

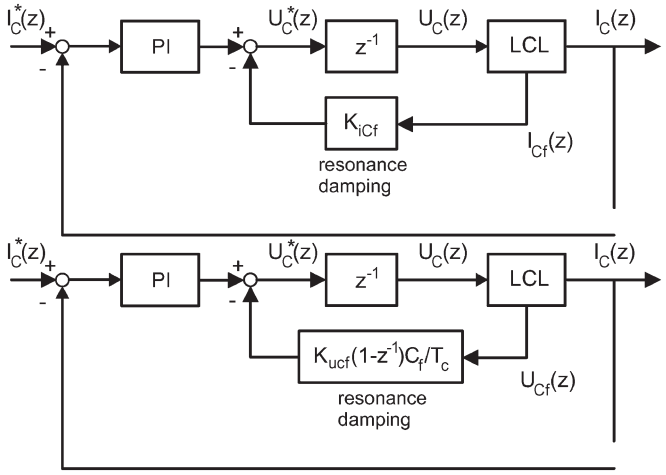

Fig. 6. Detailed current control structure: PI control with resonance damping by feedback of (top) I_{Cf} and (bottom) U_{Cf}.

one axis only. The fundamental PI controller in its backwards implementation [17] and a one sample period delay due to computation and PWM are included. A discrete control implementation of resonance damping parts are considered, whereas different feedback gains K_{iCf} and K_{uCf} are studied.

A. Filter Capacitor Current Feedback

Fig. 7 shows pole zero maps for high, medium, and low resonance frequencies. It can be seen that resonance poles can be damped into the unity circle with the proper tuning of feedback gain K_{iCf} at high and medium resonance frequencies. As discussed in Section V, resonance damping suffers from interactions with the fundamental controller if the resonance frequency gets lower. For this reason, resonance damping becomes impossible for low resonance frequencies. The dynamic response can be seen in Fig. 8 for high and medium resonance frequencies, respectively. It can be seen that, with the proper tuning of K_{iCf}, a fast response with good resonance damping is obtained.

B. Filter Capacitor Voltage Feedback

Fig. 9 shows pole zero maps for different resonance frequencies with U_{Cf} feedback. Again, the interactions with the fundamental controller make resonance damping worse at low resonance frequencies, even if it is slightly better than with I_{Cf} feedback in this case. Due to the discrete implementation, there is a difference between derivative U_{Cf} feedback and proportional I_{Cf} feedback, even though $I_{Cf}(s) = sC_fU_{Cf}(s)$ holds in the continuous domain. As discussed in Section V, the characteristics of the differentiator change to proportional gain at higher frequencies (see Fig. 5). As proportional U_{Cf} feedback cannot provide damping (see Fig. 4), no resonance damping is obtained at higher resonance frequencies, as can be seen in Fig. 9 (left).

Fig. 10 shows the step responses at medium and low resonance frequencies. Proper tuning yields resonance damping. However, at low resonance frequency, the resonance oscillations decay more slowly. Higher feedback gain K_{uCf} cannot

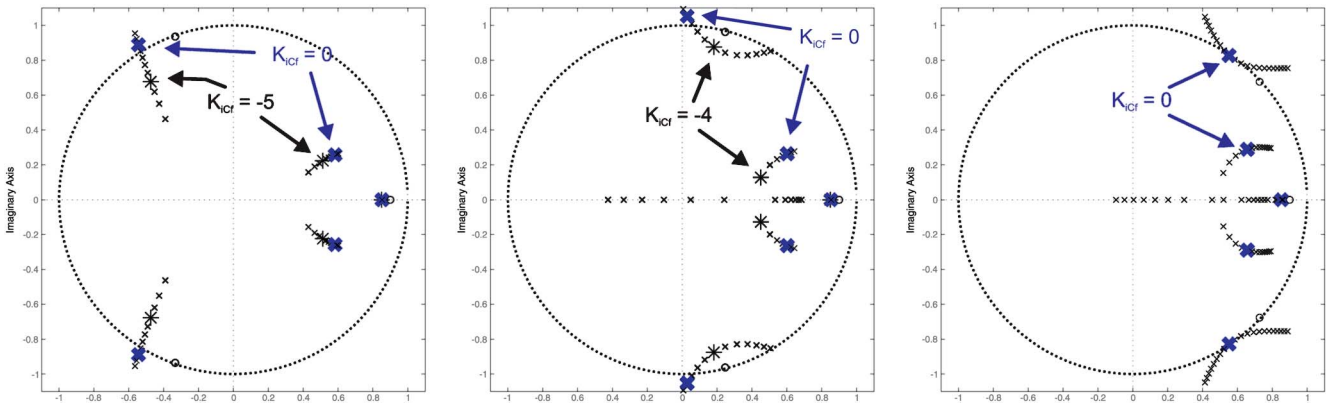

Fig. 7. I_{Cf} feedback: Impact of feedback gain K_{iCf} on the pole zero map for LCL filters with different resonance frequencies: (left) $f_{\mathrm{Res}} = 1.69$ kHz; (middle) $f_{\mathrm{Res}} = 1.19$ kHz; (right) $f_{\mathrm{Res}} = 0.69$ kHz.

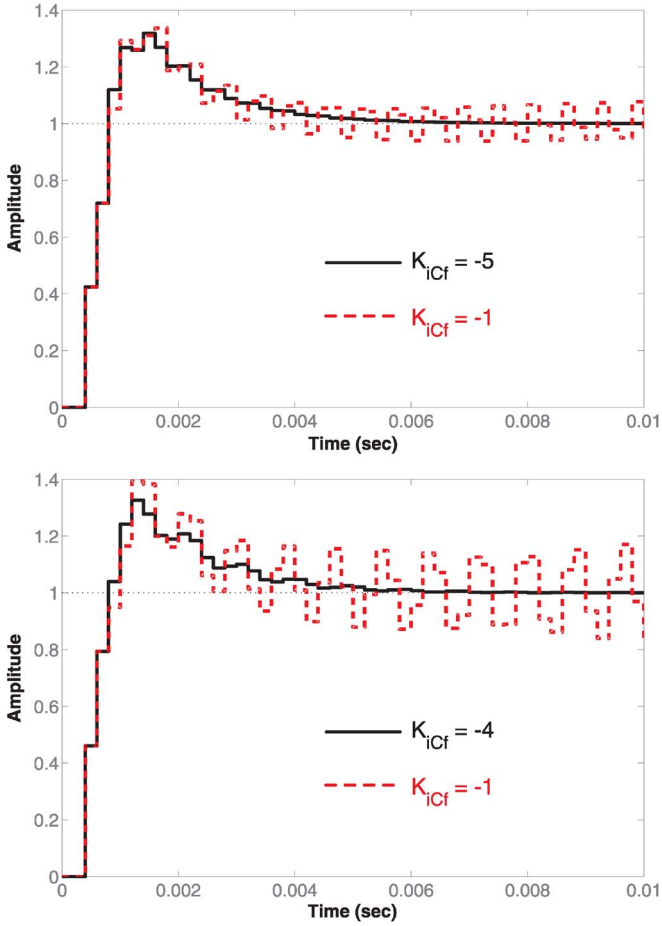

Fig. 8. I_{Cf} feedback: Impact of feedback gain K_{iCf} on the step response for LCL filters with different resonance frequencies: (top) $f_{\mathrm{Res}} = 1.69$ kHz and (bottom) $f_{\mathrm{Res}} = 1.19$ kHz.

improve damping, but instead poles are pushed outside again, as can be seen in Fig. 9 (right).

VII. Measurement Results

In order to validate the theoretical analysis, measurements have been carried out on a laboratory test setup with a self-built back-to-back converter feeding a 22 kW induction motor. See Table II for the relevant system settings. The control algorithm is implemented on a dSPACE DS 1006 board and executed twice per switching period. Unless otherwise stated, tests are carried out with a motor speed of 1000 r/min. The load torque generated by a dc machine is adjusted in order to obtain a constant active power of 10 kW on the grid side. Current reference steps are applied to the reactive current component in order to test the dynamic behavior. In the steady state, a reactive power of 10 kVA is supplied to the grid. Harmonic compensators on the grid side, as shown in [24], are not used here.

Due to parasitic damping, the LCL resonance poles are naturally damped [9]. In order to clearly excite the LCL resonance also in the steady state, the PI gain is slightly increased by 20%. The response of the PI-controlled system without feedback of any filter capacitor signal is shown in Fig. 11 and the steady state current spectra are shown in Fig. 14 (left). The currents are much distorted by the system resonance at 1.2 kHz. However, low frequency distortions due to 5th and 7th line voltage harmonics are also visible.

The results obtained with resonance damping are shown in Figs. 12 and 14 (middle) for I_{Cf} feedback and in Figs. 13 and 14 (right) for U_{Cf} feedback, respectively. A fast dynamic can be seen in the step responses. There are more oscillations visible in the line-side current and there is coupling between the d- and q-axis. The resonance is well damped, but the currents are still distorted by the low frequency line voltage harmonics. Note that harmonic compensators could reduce these distortions.

VIII. Comparison

Table IV gives a summary of the results. The basic study in Section IV shows that proportional feedback is required for I_{Cf} feedback and derivative feedback for U_{Cf} feedback. Note that no significant distortion problem occurred due to the amplification of high frequencies by derivative feedback.

The detailed analysis in Section VI shows that the behavior of the approaches adopted depends on the ratio of resonance frequency to control frequency. At high resonance frequencies, only current feedback can stabilize the system. At medium resonance frequencies, both approaches show good performance. In general, the interactions of resonance poles with the dominant low frequency pole pair are higher with U_{Cf} feedback. Hence, step responses are slightly more oscillatory. At low resonance frequencies, stability gets worse even though voltage feedback

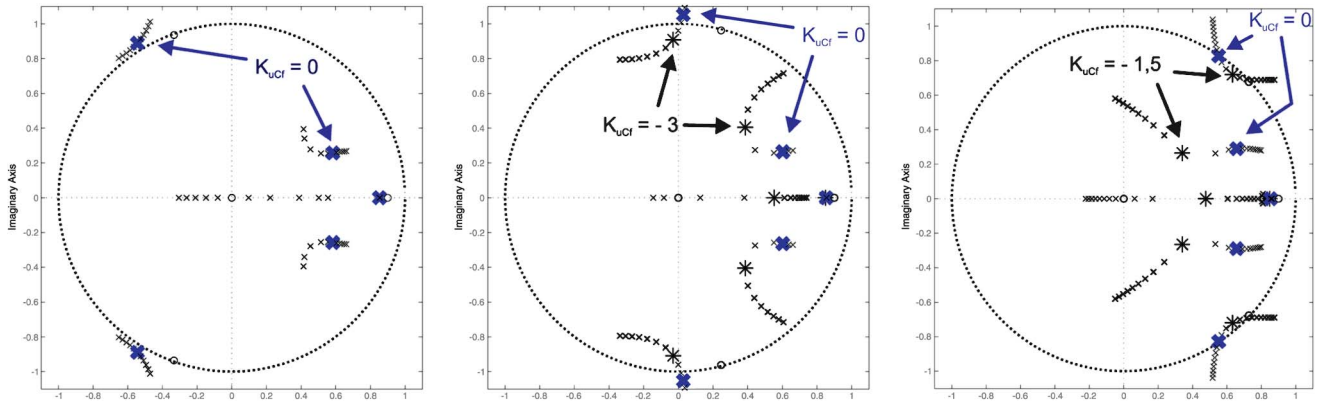

Fig. 9. U_{Cf} feedback: Impact of feedback gain K_{uCf} on the pole zero map for LCL filters with different resonance frequencies: (left) $f_{\mathrm{Res}} = 1.69$ kHz; (middle) $f_{\mathrm{Res}} = 1.19$ kHz; (right) $f_{\mathrm{Res}} = 0.69$ kHz.

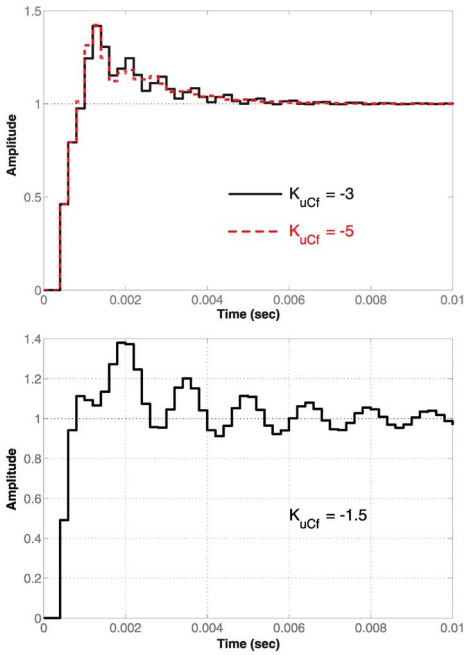

Fig. 10. U_{Cf} feedback: Impact of feedback gain K_{uCf} on the step response for LCL filters with different resonance frequencies: (top) $f_{\mathrm{Res}} = 1.19$ kHz and (bottom) $f_{\mathrm{Res}} = 0.69$ kHz.

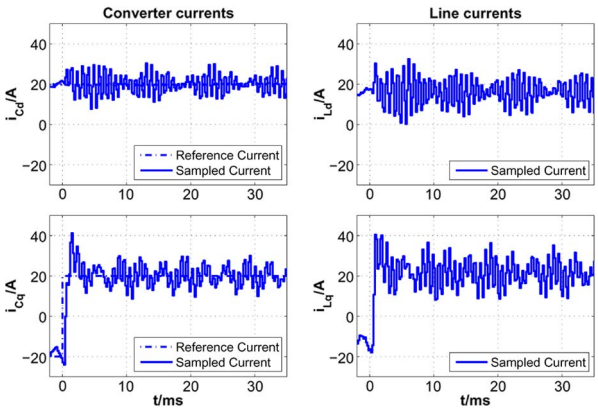

Fig. 11. PI control without feedback of either I_{Cf} or U_{Cf}: measured step response of (left) dq converter current and (right) line current at medium resonance frequency.

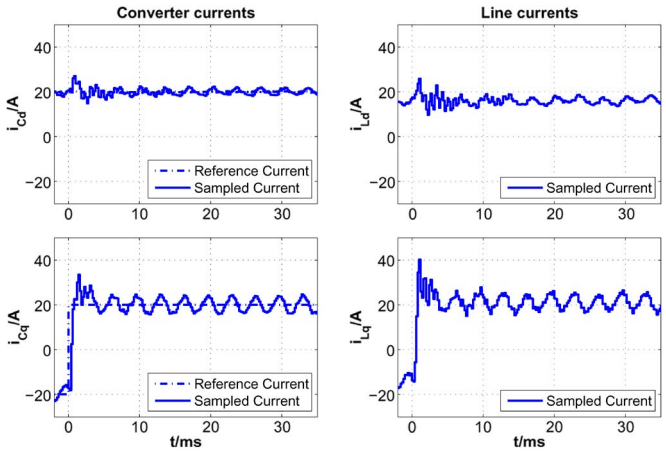

Fig. 12. I_{Cf} feedback: measured step response of (left) dq converter current (right) and line current at medium resonance frequency.

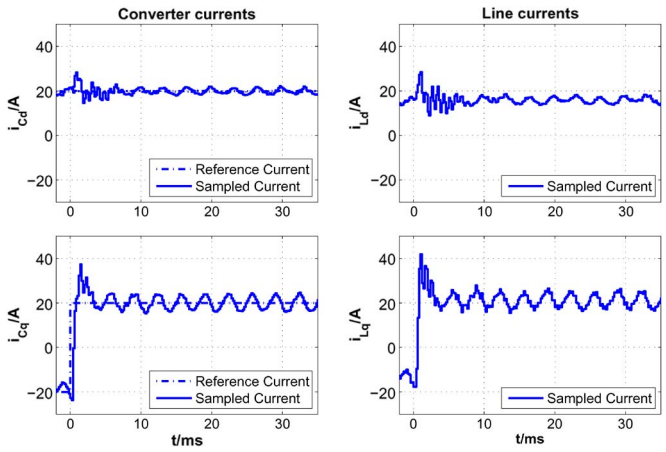

Fig. 13. U_{Cf} feedback: measured step response of (left) dq converter current and (right) line current at medium resonance frequency.

offers better damping properties. Anyway, when the ratios are too low, both approaches yield instability.

IX. Conclusion

In this paper, the LCL resonance properties of the filter capacitor current and voltage have been analyzed. A basic study shows that either proportional feedback of the currents through

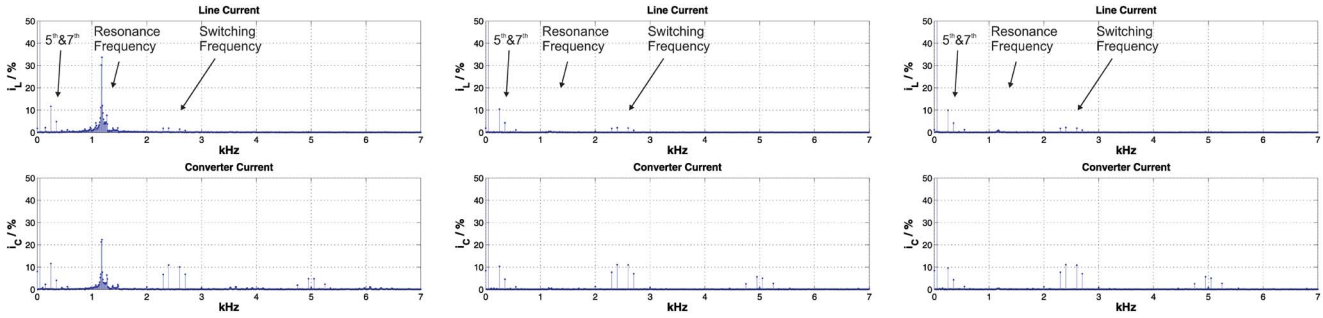

Fig. 14. Measured steady state spectra of (top) phase line currents and (bottom) converter currents for medium resonance frequency (left) without any additional feedback, (middle) I_{Cf} feedback, and (right) U_{Cf} feedback (sampling frequency: 100 kHz).

TABLE IV
COMPARISON OF I_{Cf} AND U_{Cf} FEEDBACK

	I_{Cf} feedback	U_{Cf} feedback
Required feedback	proportional	derivative
Higher ratios f_{Res}/f_c	++	–
Medium ratios f_{Res}/f_c	+	+
Lower ratios f_{Res}/f_c	–	0

the LCL filter capacitors or derivative feedback of the voltages across them is required to stabilize the system. A detailed analysis with detailed discrete models also addresses practical issues. Moreover, limitations in damping capability of the selected approaches have been revealed when different LCL filter settings are considered. The typical range of filter settings has been covered in the analysis. Even though three characteristic settings are considered in the detailed study, the results can easily be transferred to other particular settings, with other parameters. For different ratios of resonance frequency and control frequency, the selected approaches behave differently. Experimental tests on a medium power drive in a laboratory have validated the theoretical results.

In future works, it can be investigated whether systems, even with low LCL resonance frequencies, can be made stable by feeding back both the current through and voltage across the filter capacitors. Roughly speaking, proportional voltage feedback is used for shifting the frequency into the frequency range in which current feedback achieves resonance damping. However, as the complete LCL filter state vector needs to be known anyway, state space control approaches can be applied as well. In contrast to the manual tuning of two damping parameters, pole placement design offers a straightforward design procedure and the possibility of specifying the desired closed-loop pole-zero locations. Estimation of certain system states could reduce the effort required of the sensor. For example, the derivation of filter capacitor voltage is a simple method for estimating filter capacitor current.

REFERENCES

[1] M. P. Kazmierkowski, R. Krishnan, and F. Blaabjerg, *Control in Power Electronics: Selected Problems*. Oxford, U.K.: Academic, 2002.

[2] F. Blaabjerg, R. Teodorescu, M. Liserre, and A. Timbus, "Overview of control and grid synchronization for distributed power generation systems," *IEEE Trans. Ind. Electron.*, vol. 53, no. 5, pp. 1398–1409, Oct. 2006.

[3] V. Blasko and V. Kaura, "A novel control to actively damp resonance in input LC filter of a three-phase voltage source converter," *IEEE Trans. Ind. Appl.*, vol. 33, no. 2, pp. 542–550, Mar./Apr. 1997.

[4] M. Malinowski and S. Bernet, "A simple voltage sensorless active damping scheme for three-phase PWM converters with an LCL filter," *IEEE Trans. Ind. Electron.*, vol. 55, no. 4, pp. 1876–1880, Apr. 2008.

[5] M. Liserre, R. Teodorescu, and F. Blaabjerg, "Stability of photovoltaic and wind turbine grid-connected inverters for a large set of grid impedance values," *IEEE Trans. Power Electron.*, vol. 21, no. 1, pp. 263–272, Jan. 2006.

[6] E. Wu and P. Lehn, "Digital current control of a voltage source converter with active damping of LCL resonance," *IEEE Trans. Power Electron.*, vol. 21, no. 5, pp. 1364–1373, Sep. 2006.

[7] P. A. Dahono, "A control method to damp oscillation in the input LC filter," in *Proc. IEEE Power Electron. Spec. Conf.*, 2002, vol. 4, pp. 1630–1635.

[8] J. Dannehl, F. Fuchs, and S. Hansen, "PWM rectifier with LCL-filter using different current control structures," in *Proc. Eur. Conf. Power Electron. Appl.*, Sep. 2007, pp. 1–10.

[9] J. Dannehl, C. Wessels, and F. Fuchs, "Limitations of voltage-oriented PI current control of grid-connected PWM rectifiers with LCL filters," *IEEE Trans. Ind. Electron.*, vol. 56, no. 2, pp. 380–388, Feb. 2009.

[10] M. Liserre, A. Dell'Aquila, and F. Blaabjerg, "Stability improvements of an LCL-filter based three-phase active rectifier," in *Proc. 33rd Annu. IEEE PESC*, 2002, vol. 3, pp. 1195–1201.

[11] M. Prodanovic and T. C. Green, "Control and filter design of three-phase inverters for high power quality grid connection," *IEEE Trans. Power Electron.*, vol. 18, no. 1, pp. 373–380, Jan. 2003.

[12] E. Twining and D. G. Holmes, "Grid current regulation of a three-phase voltage source inverter with an LCL input filter," in *Proc. IEEE Power Electron. Spec. Conf.*, Jun. 23–27, 2002, vol. 3, pp. 1189–1194.

[13] L. Mihalache, "A high performance DSP controller for three-phase PWM rectifiers with ultra low input current THD under unbalanced and distorted input voltage," in *Conf. Rec. IEEE IAS Annu. Meeting*, 2005, vol. 1, pp. 138–144.

[14] C. Wessels, J. Dannehl, and F. Fuchs, "Active damping of LCL-filter resonance based on virtual resistor for PWM rectifiers—Stability analysis with different filter parameters," in *Proc. IEEE PESC*, Jun. 2008, pp. 3532–3538.

[15] D. Schröder, *Elektrische Antriebe 2, Regelung von Antriebssystemen,* 2nd ed. Berlin, Germany: Springer-Verlag, 2001.

[16] M. Liserre, F. Blaabjerg, and S. Hansen, "Design and control of an LCL-filter-based three-phase active rectifier," *IEEE Trans. Ind. Appl.*, vol. 41, no. 5, pp. 1281–1291, Sep./Oct. 2005.

[17] K. J. Aaström and B. Wittenmark, *Computer-Controlled Systems: Theory and Design,* 3rd ed. Upper Saddle River, NJ: Prentice-Hall, 1997, ser. Prentice-Hall Information and System Sciences Series.

[18] M. Liserre, A. Dell'Aquila, and F. Blaabjerg, "Genetic algorithm-based design of the active damping for an LCL-filter three-phase active rectifier," *IEEE Trans. Power Electron.*, vol. 19, no. 1, pp. 76–86, Jan. 2004.

[19] I. J. Gabe, V. F. Montagner, and H. Pinheiro, "Design and implementation of a robust current controller for VSI connected to the grid through an LCL filter," *IEEE Trans. Power Electron.*, vol. 24, no. 6, pp. 1444–1452, Jun. 2009.

[20] W.-T. Franke, J. Dannehl, F. W. Fuchs, and M. Liserre, "Characterization of differential-mode filter for grid-side converters," in *Proc. 35th IEEE IECON*, Nov. 2009, pp. 4080–4085.

[21] M. Liserre, R. Teodorescu, and F. Blaabjerg, "Multiple harmonics control for three-phase grid converter systems with the use of PI-RES current

controller in a rotating frame," *IEEE Trans. Power Electron.*, vol. 21, no. 3, pp. 836–841, May 2006.
[22] J. Dannehl, F. Fuchs, and P. Thøgersen, "PI state space current control of grid-connected PWM converters with LCL filters," in *Proc. IEEE Energy Convers. Congr. Expo.*, 2009, pp. 3915–3922.
[23] K. Jalili and S. Bernet, "Design of LCL filters of active-front-end two-level voltage-source converters," *IEEE Trans. Ind. Electron.*, vol. 56, no. 5, pp. 1674–1689, May 2009.
[24] R. Teodorescu, F. Blaabjerg, U. Borup, and M. Liserre, "A new control structure for grid-connected LCL PV inverters with zero steady-state error and selective harmonic compensation," in *Proc. IEEE Appl. Power Electron. Conf. Expo.*, 2004, vol. 1, pp. 580–586.

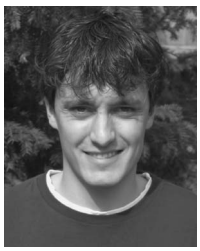

Jörg Dannehl (S'06) was born in Flensburg, Germany, in 1980. He received the Dipl. Ing. degree from Christian-Albrechts-University of Kiel, Kiel, Germany, in 2005.

Since 2005, he has been a Research Assistant at the Institute for Power Electronics and Electrical Drives, Christian-Albrechts-University of Kiel. His main research interests are control of power converters and drives.

Mr. Dannehl is student member of the IEEE Industrial Electronics Society, IEEE Power Electronics Society, and VDE.

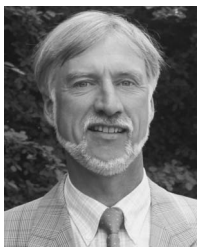

Friedrich Wilhelm Fuchs (M'96–SM'01) received the Dipl. Ing. and Ph.D. degrees from RWTH Aachen University, Aachen, Germany, in 1975 and 1982, respectively.

In 1975, he carried out research work on ac automotive drives at RWTH Aachen University. Between 1982 and 1991, he was Group Manager for the development of power electronics and electrical drives for a medium-sized company. In 1991, he joined the Converter and Drives Division, AEG (currently Converteam), Berlin, Germany, where he was the Managing Director for research, design, and development of drive products, drive systems, and high-power supplies, covering the power range from 5 kVA to 50 MVA. In 1996, he joined the Christian-Albrechts-University of Kiel, Kiel, Germany, as a Full Professor and Head of the Institute for Power Electronics and Electrical Drives. His research interests are power semiconductor applications, converter topologies, variable-speed drives, as well as their control. There is special focus on renewable energy conversion, particularly wind and solar energy, on nonlinear control of drives, as well as on diagnosis of drives and fault-tolerant drives. Many research projects are carried out with industrial partners. His institute is a member of CEwind e.G., registered corporative, competence center of research in universities in wind energy Schleswig-Holstein, as well as of KLSH, competence center for power electronics Schleswig-Holstein. He has authored or coauthored more than 150 papers.

Dr. Fuchs is Chairman of the supervisory board of Cewind, convenor (DKE, IEC), international speaker for standardization of power electronics, and a member of VDE and EPE.

Steffan Hansen (S'95–A'96–M'99) was born in Sonderborg, Denmark, in 1971. He received the M.Sc.E.E. degree from Aalborg University, Aalborg, Denmark, in 1996, and the Ph.D. degree, through an industrial fellowship supported by Danfoss Drives A/S, Graasten, Denmark and the Danish Academy of Technical Sciences, from the same university in 2001.

He is currently the Director of Technology for Danfoss Drives A/S, where he has held various positions since 1996. His research interests include solutions to reduce line-side harmonics from adjustable-speed drives, control engineering of adjustable-speed drives, and their applications.

Paul Bach Thøgersen (M'92–SM'01) was born in Thy, Denmark, on June 29, 1959. He received the M.Sc.E.E. degree in control engineering and the Ph.D. degree in power electronics and drives from Aalborg University, Aalborg, Denmark, in 1984 and 1989, respectively.

From 1988 to 1991, he was an Assistant Professor at Aalborg University. From 1991 to 2005, he was with Danfoss Drives A/S, Graasten, Denmark, first as a Research and Development Engineer and later as Manager of Technology, mainly responsible for the drives control technology area. Since 2006, he has been the Manager of the Modeling and Control Group, R&D Department, KK Electronic, Aalborg. Since 1991, he has kept a close relationship with Aalborg University, resulting in more than 20 coauthored papers and participation in more than ten Ph.D. student advisory groups.

Dr. Thøgersen was the recipient of the Angelo Award in 1999 for his contributions to the development of industrial drives.